NOAA Technical Memorandum ERL AOML-38

ON SURFACE GRAVITY WAVE SPECTRA OBSERVED IN A MOVING FRAME OF REFERENCE

Robert Bryan Long

Atlantic Oceanographic and Meteorological Laboratories
Miami, Florida
June 1979

NATIONAL OCEANIC AND ATMOSPHERIC ADMINISTRATION / Environmental Research Laboratories

NOAA Technical Memorandum ERL AOML-38

ON SURFACE GRAVITY WAVE SPECTRA OBSERVED IN A MOVING FRAME OF REFERENCE

Robert Bryan Long

Atlantic Oceanographic and Meteorological Laboratories
Miami, Florida
June 1979

UNITED STATES
DEPARTMENT OF COMMERCE
Juanita M. Kreps, Secretary

NATIONAL OCEANIC AND
ATMOSPHERIC ADMINISTRATION
Richard A. Frank, Administrator

Environmental Research
Laboratories
Wilmot N. Hess, Director

CONTENTS

On Surface Gravity Wave Spectra Observed in a Moving Frame of Reference

Robert Bryan Long

Abstract. Spectral analyses of one- or two-dimensional records of sea surface elevation yield one- or two-dimensional encounter spectra that are, in fact, weighted integrals over the two-dimensional surface wave spectrum. These integral relationships are determined by the type of record and the motion of the observer relative to the water on which the waves are running. We derive the relevant relationships for uniform translation of the observer at arbitrary velocity and for arrays of discrete or linearly distributed sensors. The problem of estimating the wave spectrum, given the encounter spectrum, is considered in detail for the two cases exemplified by a wave gage array in a current and by a side-looking surface-imaging radar.

1. INTRODUCTION

A classic procedure for observing ocean wave spectra is to place wave gages in the sea to obtain time series of surface elevation from which various moments of the full two-dimensional surface wave spectrum may be estimated. This procedure has in recent years been augmented by several remote-sensing techniques (e.g., airborne radar and laser altimeters, stereophotography, side-looking imaging radars, etc.), each of which provides information on some moment of the full two-dimensional

spectrum. The nature of the moment is determined by the type of observation (discrete or distributed sensors, as defined in the following sections) and the motion of the observer relative to the water on which the waves are running. These relationships have been worked out in detail for several specific cases: for fixed instruments and stereophotography, see, e.g., Kinsman (1965) and references there; for non-scanning laser/radar altimeters, the relevant theory is developed in the context of shipborne wave gages by St. Denis and Pierson (1953) and in Cartwright (1963); for a scanning laser altimeter translating at large velocity, see Snyder (1973); for surface-imaging devices, such as side-looking radars, translating at large velocity, see Pierson (1975). The type of observations produced by surface-imaging devices translating at arbitrary velocity has not been treated in adequate detail, nor has the problem of wave gage arrays in a current. This paper presents a unified formulation within which all the above examples appear as special cases. The generality of the results is restricted only by the requirement that the motion of the observer be limited to translation at constant velocity and that distributed sensors be distributed along straight lines.

2. FORMULATING THE PROBLEM

We consider the sea surface elevation, ζ, to be a Gaussian random function of the three-dimensional vector, $\bar{x}(x,y,t)$, where x and y are horizontal space coordinates and t (the "vertical" coordinate) is time. The statistics of $\zeta(\bar{x})$ are taken to be homogeneous and stationary; hence, ensemble averages (indicated here by angle brackets $< >$) are independent of $\bar{x}$. These statistics have the general form

$$C_{\zeta^{n+1}}(\bar{\rho}_1,\bar{\rho}_2,\ldots,\bar{\rho}_n)=<\zeta(\bar{x})\zeta(\bar{x}+\bar{\rho}_1)\ldots\zeta(\bar{x}+\bar{\rho}_n)>,$$

i.e., mean lagged products of order n+1. The $\bar{\rho}$'s are three-dimensional lag vectors, e.g., $\bar{\rho}=(\rho,\sigma,\tau)$. At the lowest order,

$$C_\zeta = \langle \zeta(\bar{x}) \rangle$$

is just the mean surface elevation, which we may set to zero without loss of generality. At the next order,

$$C_{\zeta 2}(\bar{\rho}) = \langle \zeta(\bar{x}) \zeta(\bar{x}+\bar{\rho}) \rangle \tag{2.1}$$

is the covariance function. For a Gaussian process, the statistics are completely specified by these two averages, and we need not consider higher order mean products.

The wave spectrum is the three-dimensional Fourier transform of the covariance function, viz.,

$$F(\bar{K}) = \int d\bar{\rho} C_{\zeta 2}(\bar{\rho}) e^{-i\bar{k}\cdot\bar{\rho}} \tag{2.2}$$

where $\bar{K}=(K_x,K_y,f)$, $\bar{k}\equiv 2\pi\bar{K}=(k_x,k_y,\omega)$, and

$$\int d\bar{\rho}\ldots \equiv \int_{-\infty}^{\infty}\int\int d\rho d\sigma d\tau \ldots .$$

The inverse transform is

$$C_{\zeta 2}(\bar{\rho}) = \int d\bar{K} F(\bar{K}) e^{i\bar{k}\cdot\bar{\rho}} \tag{2.3}$$

where

$$\int d\bar{K}\ldots \equiv \int_{-\infty}^{\infty}\int\int dK_x dK_y df \ldots .$$

We note from (2.1) that $C_{\zeta 2}(0)$ is the mean square surface displacement. From (2.3) with $\bar{\rho}=0$, we conclude that $dK_x dK_y df F(\bar{K})$ may be interpreted as

the contribution to mean square surface displacement due to the complex surface wave component with wave number vector $\bar{K}$.

Thus, corresponding to the random function, ζ, defined in physical space, $\bar{x}$, we have the covariance function, $C_{\zeta 2}$, defined in lag space, $\bar{\rho}$, and the spectrum defined in wave number space, $\bar{K}$. We have treated the wave spectrum so far as though it were fully three-dimensional. In fact, the physics of small-amplitude surface gravity waves prohibits the existence of waves at wave numbers not satisfying the dispersion relation, which has the form

$$f=\pm\Omega(K)$$

where $K\equiv(K_x^2+K_y^2)^{\frac{1}{2}}$. This constraint reduces the region in $\bar{K}$ space where F is non-zero from three to two dimensions. We shall incorporate the dispersion constraint later, but for the moment it is convenient to ignore it and continue to treat the spectrum as though it were fully three-dimensional.

The discussion above assumes that the complete data set is available, i.e., that we have all the realizations of $\zeta(\bar{x})$ for all $\bar{x}$. No physically realizable experiment can provide such extensive data. The limitations can be separated into three categories: (a) instruments generally provide knowledge of $\zeta(\bar{x})$ only along curves or on surfaces in (x,y,t) space, (b) these regions cannot extend to infinity, and (c) we generally have only a few such finite realizations of the process to work with. The effect of (b) and (c) is to limit the resolution and precision with which the wave spectrum can be estimated from a given sample of data, a topic widely explored in the literature and, hence, of no concern to us here. We shall ignore (b) and (c) and focus our attention on (a).

Limiting the available knowledge of $\zeta(\bar{x})$ to some subspace of (x,y,t) results in a corresponding limitation on knowledge of $C_{\zeta 2}(\bar{\rho})$.

Consequently, it is not possible under these conditions to carry out the three-fold integration necessary to transform $C_{\zeta 2}$ into F. However if we restrict sensor motion to translation at constant velocity, there exists at least one direction in (x,y,t) and, consequently, in (ρ,σ,τ), along which one dimension of a Fourier transformation may be carried out. If, further, the sensor is distributed along a straight line (i.e., measures ζ along an instantaneous profile rather than at an instantaneous point), two dimensions of Fourier transformation may be carried out. These operations yield one- or two-dimensional encounter spectra; the integral relationships between these encounter spectra and the full three-dimensional surface wave spectrum are the objects of primary interest in the next two sections.

3. THE EFFECT OF LIMITED DATA: DISCRETE SENSORS

Consider now the case of J discrete surface elevation sensors maintained in a rigid geometry relative to each other and undergoing translation at constant velocity relative to the water on which the waves are running. Examples of this type of experiment include arrays of bottom-mounted wave gages in the presence of a current and non-scanning airborne laser or radar altimeters. We can, without loss of generality, let (U,0) be the translation velocity vector, i.e., specify the translation to be in the x direction.

Such an experiment can provide information on $\zeta(\bar{x})$ only along the J parallel lines in (x,y,t) defined by the constraints

$$\left.\begin{aligned} x &= Ut + x_j \\ y &= y_j \end{aligned}\right\} \; j=1,2,\ldots,J$$

where x_j and y_j are the spatial coordinates of the j^{th} sensor at t=0

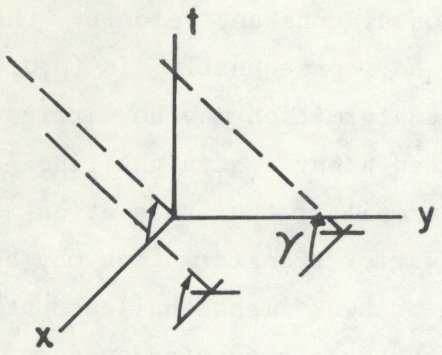

Figure 1a. Geometry of the discrete sensor problem. Figure 1a shows data lines in physical space for a three-element discrete sensor array translating along x at U=cot(γ). Only the positive t half space is shown.

(see Fig. 1a). We are free to take either x or t as the independent variable defining the data lines. The choice we make determines whether we arrive at the encounter frequency spectrum or an encounter wave number spectrum as the relevant statistic of the data. Both representations are needed if we are to consider the full range of translation speeds $0 \leq U \leq \infty$.

In the present case, then, the data subspace is defined by either

$$\bar{x}=(Ut+x_j,y_j,t)\equiv\bar{x}_j(t) \tag{3.1}$$

or, equivalently,

$$\bar{x}=(x,y_j,\frac{x}{U}+t_j)\equiv\bar{x}_j(x) \tag{3.2}$$

where $t_j=-\frac{1}{U}x_j$. With such limited knowledge of ζ, we can compute the covariance function only for a limited region in lag space. Specifically, we have from (3.1)

$$C_{\zeta 2}(\bar{\rho}_i(\tau))=<\zeta(\bar{x}_j(t))\zeta(\bar{x}_k(t+\tau))> \tag{3.3}$$

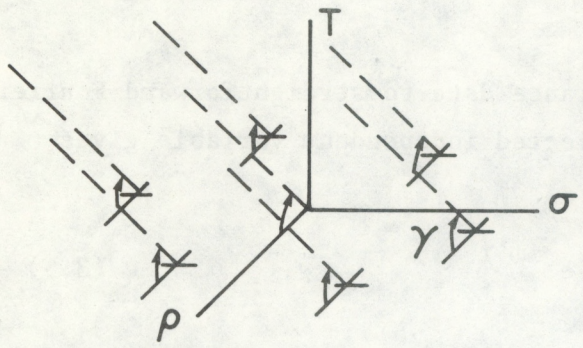

Figure 1b. Geometry of the discrete sensor problem (cont.). Figure 1b shows covariance lines in lag space corresponding to the data lines in Fig. 1a. Only the positive τ half space is shown.

where

$$\bar{\rho}_i(\tau)=(U\tau+\rho_i,\sigma_i,\tau)$$

$\rho_i=x_k-x_j$, and $\sigma_i=y_k-y_j$.

Alternately, from (3.2) we may write

$$C_{\zeta 2}(\bar{\rho}_i(\rho))=<\zeta(\bar{x}_j(x))\zeta(\bar{x}_k(x+\rho))> \qquad (3.4)$$

where

$$\bar{\rho}_i(\rho)=(\rho,\sigma_i,\frac{\rho}{U}+\tau_i)$$

and

$$\tau_i=t_k-t_j=-\frac{1}{U}(x_k-x_j) \quad .$$

Thus, corresponding to the J data lines in (x,y,t), there are J(J-1)+1 lines in (ρ,σ,τ) along which we know $C_{\zeta 2}$ (see Fig. 1b). Because of

the rigid geometry and uniform translation velocity (U,0), the lines are all straight, parallel, perpendicular to the y (or σ) axis, and inclined to the x (or ρ) axis at arctan $(\frac{1}{U})$.

Subjecting the available covariance data to straightforward Fourier transforming with respect to the selected independent variable gives

$$E'(f';\rho_i,\sigma_i)=\int_{-\infty}^{\infty} d\tau C_{\zeta 2}(\bar{\rho}_i(\tau))e^{-i\omega'\tau} \tag{3.5}$$

where E' is the one-dimensional encounter frequency spectrum, or alternately,

$$F'(K'_x;\sigma_i,\tau_i)=\int_{-\infty}^{\infty} d\rho C_{\zeta 2}(\bar{\rho}_i(\rho))e^{-ik'_x\rho} \tag{3.6}$$

where F' is the one-dimensional encounter wave number spectrum, and $f'\equiv\frac{1}{2\pi}\omega'$ and $K'_x\equiv\frac{1}{2\pi}k'_x$ are encounter frequency and wave number component, respectively.

We may interpret (3.5) and (3.6) as line integrals carried out along the only direction in (ρ,σ,τ) for which $C_{\zeta 2}$ is known with sufficient density to make possible integration, but with distance along the line parameterized by either τ or ρ. An alternate and, in some ways, more useful point of view is to consider Eqs. (3.1) and (3.2) to be mappings that project the data lines defined in (x,y,t) onto corresponding one-dimensional spaces (t) or (x). Each such mapping, tagged by the sensor initial coordinates (x_j,y_j), constitutes an appropriate way to display the data record produced by the j^{th} sensor. Eqs. (3.3) and (3.4) are then equivalent to computing the covariance between these one-dimensional records; equivalently, they may be interpreted as the result of mappings that project the known covariance lines in (ρ,σ,τ) onto corresponding one-dimensional lag spaces (τ) or (ρ), each such projection being tagged by the "initial" lags (ρ_i,σ_i). From this point

of view, (3.5) and (3.6) become cross spectra between the j^{th} and k^{th} data records.

In either case, (3.5) and (3.6) are exactly equivalent to the full, three-dimensional transforms

$$E'(f';\rho_i,\sigma_i)=\int d\bar{\rho} C_{\zeta 2}(\bar{\rho})\delta(\rho-U\tau-\rho_i)$$

$$\delta(\sigma-\sigma_i)e^{-i(\bar{k}\cdot\bar{\rho}-k_x\rho_i-k_y\sigma_i)} \qquad (3.7)$$

and

$$F'(K_x';\sigma_i,\tau_i)=\int d\bar{\rho} C_{\zeta 2}(\bar{\rho})\delta(\tau-\frac{f}{U}-\tau_i)$$

$$\delta(\sigma-\sigma_i)e^{-i(\bar{k}\cdot\bar{\rho}-k_y\sigma_i-\omega\tau_i)} \qquad (3.8)$$

provided that we identify the encounter frequency as the Doppler-shifted frequency

$$f'=f+K_x U \qquad (3.9)$$

and take

$$K_x'=K_x+\frac{f}{U} \; . \qquad (3.10)$$

Note with respect to (3.9) that, with the sign convention we have used for the Fourier transform kernel, $\exp[i(k_x\rho+k_y\sigma+\omega\tau)]$, positive f implies wave propagation in the direction opposite to the vector (K_x,K_y). We may now use (2.3) for $C_{\zeta 2}(\bar{\rho})$, and then execute the integrations over $\bar{\rho}$. We get, after some manipulation,

$$E'(f;\rho_i,\sigma_i)=\int d\bar{K}F(\bar{K})\delta(f'-f-K_xU)$$

$$e^{i(k_x\rho_i+k_y\sigma_i)} \qquad (3.11)$$

and

$$F'(K_x';\sigma_i,\tau_i)=\int d\bar{K}F(\bar{K})\delta(K_x'-K_x-\frac{f}{U})$$

$$e^{i(k_y\sigma_i+\omega\tau_i)} \qquad (3.12)$$

where we have used the fact that, for any u and v,

$$\delta(u)=\int_{-\infty}^{\infty}dve^{\pm i2\pi vu} \ .$$

Thus, the encounter spectrum represents a weighted integral property of the full three-dimensional spectrum, the integration being over the plane in (K_x,K_y,f) space defined by the delta function in the integrand. The plane is parallel to the K_y axis and inclined to the K_x axis at arctan (-U), i.e., it is perpendicular in $\bar{K}$ to the direction of the data lines in $\bar{x}$ and the covariance lines in $\bar{\rho}$ (see Fig. 1c). In the limit U→0, the plane becomes "horizontal" in $\bar{K}$ space, whence $E'(f';\rho_i,\sigma_i)$ becomes the summed effect of all waves with f=f', regardless of wavelength or propagation direction; $F'(K_x';\sigma_i,\tau_i)$ becomes meaningless in this limit. As U→∞, the plane becomes "vertical," and $F'(K_x';\sigma_i,\tau_i)$ becomes the summed effect of all waves with $K_x=K_x'$, regardless of frequency or propagation direction; in this limit, $E'(f';\rho_i\sigma_i)$ becomes meaningless. For any finite, non-zero U, both E' and F' are equally valid representations.

We need now to incorporate the constraint of dispersion, but before doing so, we consider the case of linearly distributed sensors in the next section.

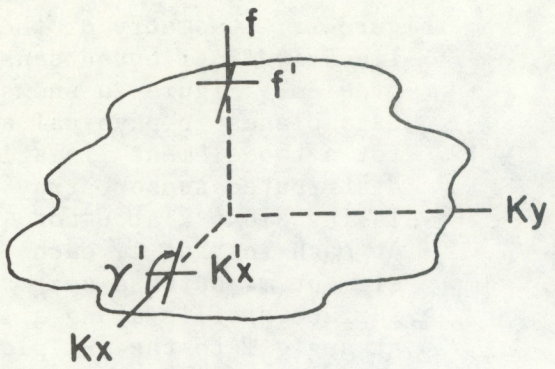

Figure 1c. Geometry of the discrete sensor problem (cont.). Figure 1c shows a patch of the encounter plane in wave number space corresponding to Figure 1a. Contributions to encounter spectra at f' (or $K'_{\bar{x}}$) arise from all surface wave numbers lying in the plane. The angle γ'=arctan (-U).

4. THE EFFECT OF LIMITED DATA: LINEARLY DISTRIBUTED SENSORS

Suppose, now, that each sensor in an array such as we considered above measures an essentially instantaneous profile of surface elevation along a straight line at angle Ψ to the y axis (instead of instantaneous surface elevation at a point). We could approximate such an experiment by arranging a field of bottom-mounted wave gages into a set of parallel, dense, line arrays. A more relevant example might be a rigidly maintained formation of aircraft carrying laterally scanning radar or laser latimeters or side-looking imaging radars, flying over the sea in the presence of a crosswind that causes heading to be displaced by an angle Ψ from the direction of the groundspeed vector (U,0). (To be precise, the imaging radars sense variations in radar reflectivity of the sea surface, not surface elevation. These variations are, however, demonstrably related to the surface wave field, although the nature of the relationship is not yet fully understood and is an area of active research at this time.)

Now, the set of data lines in $\bar{x}$ associated with the previous array of discrete sensors is replaced by a set of data planes (see Fig. 2a), each defined by the following relationship:

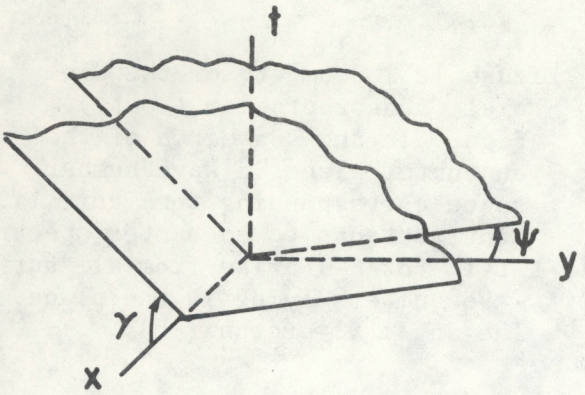

Figure 2a. Geometry of the linearly distributed sensor problem. Figure 2a shows data planes in physical space for a two-element linearly distributed sensor array translating along x at U=cot γ. At each instant t, each element measures a sea surface profile along a line at angle Ψ to the y-t plane. Only the positive y/positive t quarter space is shown.

$$x-x_j+(y-y_j)\tan\Psi=Ut, \qquad (4.1)$$

where (x_j,y_j) are the coordinates of the down-track centerline of the j^{th} data plane at t=0 (e.g., the t=0 coordinate of the j^{th} aircraft in the example above). We have three choices for independent variable pairs in (4.1), viz., (x,t), (y,t), or (x,y), each choice equivalent to projection of the data plane in (x,y,t) onto the corresponding two-dimensional subspace. Each such mapping, tagged by the initial coordinates (x_j,y_j), constitutes an appropriate way to display the two-dimensional data record produced by the j^{th} sensor. Cross-spectral analysis of the resulting "images" yields two-dimensional encounter spectra. Under limiting conditions U→0 or ∞, or tan Ψ→0 or ±∞, one or two of the three encounter spectra become meaningless; for this reason, we consider all three possibilities in parallel. (Although we could treat one of the three possibilities, and then derive the transformations necessary to obtain the other two results from the one, the level of effort would be about the same as we shall require below.)

This type of experiment, then, provides knowledge of $\zeta(\bar{x})$ only on the parallel planes in (x,y,t) defined equivalently by

$$\bar{x}=(x,(Ut-x+x_j)/\tan\Psi+y_j,t)\equiv\bar{x}_j(x,t),$$

$$\bar{x}=(Ut-(y-y_j)\tan\Psi+x_j,y,t)\equiv\bar{x}_j(y,t),$$

or

$$\bar{x}=(x,y,(x-x_j+(y-y_j)\tan\Psi)/U)\equiv\bar{x}_j(x,y)\ .$$

With such limited information, we can compute the covariance function only in a limited region in (ρ,σ,τ); specifically, we have

$$C_{\zeta 2}(\bar{\rho}_i(\rho,\tau))=<\zeta(\bar{x}_j(x,t))\zeta(\bar{x}_k(x+\rho,t+\tau))>$$

where

$$\bar{\rho}_i(\rho,\tau)=(\rho,\ \frac{U\tau-\rho}{\tan\Psi}+\sigma_i,\tau),$$

and

$$\sigma_i=\frac{x_k-x_j}{\tan\Psi}+y_k-y_j$$

is the displacement in the y direction from the j^{th} to the k^{th} data plane. Alternately, we can write

$$C_{\zeta 2}(\bar{\rho}_i(\sigma,\tau))=<\zeta(\bar{x}_j(y,t))\zeta(\bar{x}_k(y+\sigma,t+\tau))>$$

where

$$\bar{\rho}_i(\sigma,\tau)=(U\tau-\sigma\tan\Psi+\rho_i,\sigma,\tau),$$

and

$$\rho_i=x_k-x_j+(y_k-y_j)\tan\Psi$$

is the displacement in the x direction from the j^{th} to the k^{th} data plane. Finally, we may choose

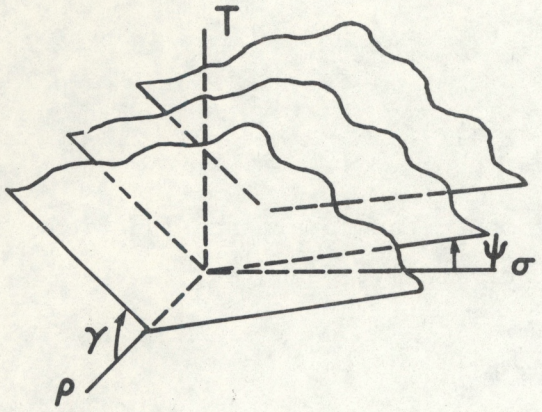

Figure 2b. Geometry of the linearly distributed sensor problem (cont.). Figure 2b shows covariance planes in lag space corresponding to the data planes in Fig. 2a. Only the positive σ/positive τ quarter space is shown.

$$C_{\zeta 2}(\bar{\rho}_i(\rho,\sigma))=\langle\zeta(\bar{x}_j(x,y))\zeta(\bar{x}_k(x+\rho,y+\sigma))\rangle,$$

where

$$\bar{\rho}_i(\rho,\sigma)=(\rho,\sigma,\frac{\rho+\sigma\ \tan\ \Psi}{U}+\tau_i),$$

and

$$\tau_i=\frac{1}{U}(-x_k+x_j-(y_k-y_j)\ \tan\ \Psi)$$

is the displacement in the t direction from the j^{th} to the k^{th} data plane.

Thus, corresponding to the data planes in $\bar{x}$, there is a set of planes in $\bar{\rho}$ on which we know the covariance (see Fig. 2b). These may be specified by any pair of the three variables, ρ,σ,τ. The choice of a pair effectively maps the covariance planes into the corresponding two-dimensional subspace; alternately, we may consider the lag-variable pair to be the consequence of the covariance having been computed between the projected images of the data planes.

In any case, transforming each of the three versions of $C_{\zeta 2}$ with respect to the chosen pair of independent lag variables is exactly equivalent to the full three-dimensional transforms

$$D''(f',K_x';\sigma_i)=\int d\bar{\rho} C_{\zeta 2}(\bar{\rho})\delta(\sigma-\frac{U\tau-\rho}{\tan\Psi}-\sigma_i)$$
$$e^{-i(\bar{k}\cdot\bar{\rho}-k_y\sigma_i)}$$

where

$$f'=f+\frac{K_y U}{\tan\Psi}$$

and

$$K_x'=K_x-\frac{K_y}{\tan\Psi} \quad ,$$

or

$$E''(f',K_y';\rho_i)=\int d\bar{\rho} C_{\zeta 2}(\bar{\rho})\delta(\rho-U\tau+\sigma\tan\Psi-\rho_i)$$
$$e^{-i(\bar{k}\cdot\bar{\rho}-k_x\rho_i)}$$

where

$$f'=f+K_x U$$

and

$$K_y'=K_y-K_x\tan\Psi \quad ,$$

or

$$F''(K_x',K_y';\tau_i)=\int d\bar{\rho} C_{\zeta 2}(\bar{\rho})\delta(\tau-\frac{\rho+\sigma\tan\Psi}{U}-\tau_i)$$
$$e^{-i(\bar{k}\cdot\bar{\rho}-\omega\tau_i)}$$

where

$$K_x'=K_x+\frac{f}{U}$$

$$K_y'=K_y+\frac{f}{U}\tan\Psi \quad ,$$

the double primes indicating two-dimensional encounter spectra. Using (2.3) for $C_{\zeta 2}(\bar{\rho})$ and carrying out the integration over $\bar{\rho}$ give, after some manipulations,

$$D''(f',K_x';\sigma_i)=\int d\bar{K}F(\bar{K})\delta(K_x'-K_x+\frac{K_y}{\tan\Psi})$$

$$\delta(f'-f-\frac{K_yU}{\tan\Psi})e^{ik_y\sigma_i} \quad , \tag{4.2}$$

$$E''(f',K_y';\rho_i)=\int d\bar{K}F(\bar{K})\delta(K_y'-K_y+K_x\tan\Psi)$$

$$\delta(f'-f-K_xU)e^{ik_x\rho_i} \quad , \tag{4.3}$$

or

$$(F''K_x',K_y';\tau_i)=\int d\bar{K}F(\bar{K})\delta(K_x'-K_x-\frac{f}{U})$$

$$\delta(K_y'-K_y-\frac{f}{U}\tan\Psi)e^{i\omega\tau_i}. \tag{4.4}$$

Thus, contributions to each of the three encounter spectra arise only from surface wave numbers lying on the line in $\bar{K}$ space fixed by the intersection of the two planes defined by the pair of delta functions in the respective integrand (see Fig. 2c).

Note the properties of the three encounter spectra for limiting values of U and tan ψ. For example, when $\psi=\pm\frac{\pi}{2}$, (4.3) and (4.4) are meaningless. (This corresponds to the case of a set of dense wave gage line arrays oriented end-on to the current, a possible but not very desirable experimental arrangement.) Contributions to the encounter spectrum (4.2) then arise from all surface wave numbers lying on the "horizontal" line in $\bar{K}$ space defined by $f=f'$ and $K_x=K_x'$, regardless of K_y.

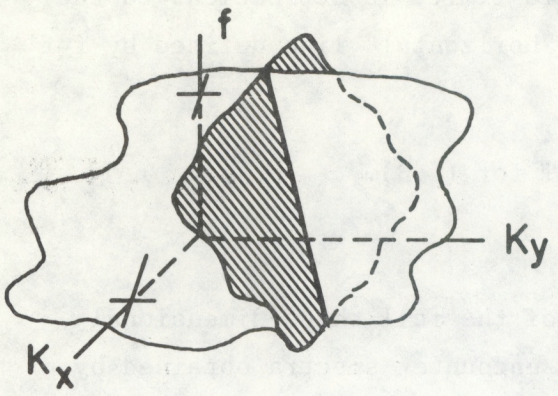

Figure 2c. Geometry of the linearly distributed sensor problem (cont.). Figure 2c shows a section of an encounter line in wave number space corresponding to Fig. 2a. Contributions to $F''(K_x',K_y',\tau_i)$ arise from all surface wave numbers lying on the intersection of the two planes defined by the two delta functions in (4.4). Although the orientation of the planes is different, similar drawings can be constructed for $D''(f',K_x';\sigma_i)$ and $E''(f',K_x';\rho_i)$.

This reflects the fact that the data, or covariance, planes are undistorted in this case by the projection onto (x,t), or (ρ,τ). When $\Psi=0$, (4.2) is meaningless; in (4.3) and (4.4), $K_y=K_y'$, reflecting the fact that the data (covariance) planes are undistorted in the cross-track direction by either of the related projections. The down-track direction corresponds to $f'=f+K_xU$ in (4.3) and $K_x'=K_x+\frac{f}{U}$ in (4.4), identical, as one would expect, to (3.9) and (3.10) for all $\Psi\neq\pm\frac{\pi}{2}$. This situation is typified by the example of the array of airborne scanning laser/radar altimeters in the absence of a crosswind (or more precisely, when the scan sweep is perpendicular to the ground track).

When $U\to\infty$, (4.2) and (4.3) become meaningless; in (4.4), $K_x'=K_x$ and $K_y'=K_y$, again reflecting the fact that in this limit the data (covariance) planes are undistorted by the projection. Contributions to the encounter spectrum arise only from the "vertical" line in $\bar{K}$ space defined by these conditions. This case is exemplified by a sequence of stereophotograph pairs taken at intervals in time corresponding to τ_i.

Finally, when $U\to 0$, (4.4) is meaningless, and for (4.2) and (4.3) $f=f'$, i.e., the down-track axis in the data (covariance) plane is

undistorted by these projections in this limit. Contributions to the encounter spectra arise only from the "horizontal" line defined by f=f' and

$$K'_x=K_x - \frac{K_y}{\tan \Psi} \text{ for (4.2)}, \quad K'_y=K_y-K_x \tan \Psi \text{ for (4.3)}.$$

We have now obtained the moments of the full three-dimensional surface wave spectrum corresponding to encounter spectra obtained by both discrete and linearly distributed sensors. For discrete sensors, the appropriate moments are surface integrals; for linearly distributed sensors the additional dimension of data reduces the appropriate moments to line integrals. We next incorporate the dispersion constraint, which further reduces the dimensions of these moments by one to line integrals for discrete sensors and to the sum of several discrete points for the linearly distributed case.

5. THE EFFECT OF SURFACE GRAVITY WAVE DISPERSION

The physics of small-amplitude surface gravity waves prohibits the existence of waves at wave numbers $\bar{K}$ not satisfying the dispersion relation

$$f=\pm\Omega(K) \tag{5.1}$$

where

$$K\equiv(K_x^{\,2}+K_y^{\,2})^{\frac{1}{2}}$$

and

$$\Omega^2=\frac{gK}{2\pi} \tanh (2\pi Kh)\approx\frac{gK}{2\pi} \quad . \tag{5.2}$$

In (5.2), h is the mean water depth, and the approximate form is accurate to ½% for h greater than $\frac{1}{2K} = \frac{1}{2}$ wavelength. Thus, contributions to integral properties of the full three-dimensional wave spectrum can arise only from the surface in $\bar{K}$ space defined by (5.1). If these integral properties are to be non-vanishing, then $F(\bar{K})$ must exhibit the characteristics of a weighted delta function located on the dispersion surface. We can make this explicit by writing

$$F(\bar{K}) \equiv F(K_x, K_y; f)\delta(f \pm \Omega) \tag{5.3}$$

where $\delta(f \pm \Omega)$ is shorthand for $[\delta(f+\Omega)+\delta(f-\Omega)]$. Then, for example, the mean square surface displacement becomes, from (2.3) with $\bar{\rho}=0$,

$$C_{\zeta^2}(0) = \int_{-\infty}^{\infty}\int dK_x dK_y [F(K_x, K_y; \Omega) + F(K_x, K_y; -\Omega)]$$

where $F(K_x, K_y; \pm\Omega)$ is the two-dimensional surface wave number spectral density for waves propagating parallel (for $-\Omega$) or antiparallel (for $+\Omega$) to the vector (K_x, K_y).

Alternately, we can, in principle , invert (5.1) to get

$$K = \kappa(f^2), \tag{5.4}$$

which we interpret as a constraint on the magnitude of (K_x, K_y), given f. This suggests the use of polar coordinates to describe $\bar{K}$ space, whence we write

$$F(\bar{K}) = \frac{1}{K} E(\theta, f; K)\delta(K - \kappa) \tag{5.5}$$

and

$$d\bar{K} = K d\theta df. \tag{5.6}$$

Then, if we use these in (2.3) with $\bar{\rho}=0$, we get the mean square surface displacement

$$C_{\zeta^2}(0)=\int_0^{2\pi} d\theta \int_{-\infty}^{\infty} df\, E(\theta,f;\kappa)$$

where $E(\theta,f;\kappa)$ is the two-dimensional wave directional frequency spectrum. We may choose θ to be the direction of the vector $(-K_x,-K_y)$; then, $d\theta df\, E(\theta,f;\kappa)$ is the contribution to mean square surface displacement due to the complex wave component with frequency f and propagation direction θ for $f>0$, $\theta+\pi$ for $f<0$. Whether we choose to specify the dispersion constraint in rectangular or polar coordinates is a question of convenience; we shall have reason to use both forms in the next section.

For the moment, we incorporate the form (5.3) into the results of Sections 3 and 4. From (3.11) and (3.12), we get for discrete sensors

$$E'(f';\rho_i,\sigma_i)=\int d\bar{K}F(K_x,K_y;f)\delta(f\pm\Omega)$$
$$\delta(f'-f-K_xU)e^{i(k_x\rho_i+k_y\sigma_i)}, \qquad (5.7)$$

and

$$F'(K_x';\sigma_i,\tau_i)=\int d\bar{K}F(K_x,K_y;f)\delta(f\pm\Omega)$$
$$\delta(K_x'-K_x-\frac{f}{U})e^{i(k_y\sigma_i+\omega\tau_i)}. \qquad (5.8)$$

From (4.2) through (4.4), we have for linearly distributed sensors

$$D''(f',K_x';\sigma_i)=\int d\bar{K}F(K_x,K_y;f)\delta(f\pm\Omega)$$
$$\delta(K_x'-K_x+\frac{K_y}{\tan\Psi})\delta(f'-f-\frac{K_yU}{\tan\Psi})e^{ik_y\sigma_i}, \qquad (5.9)$$

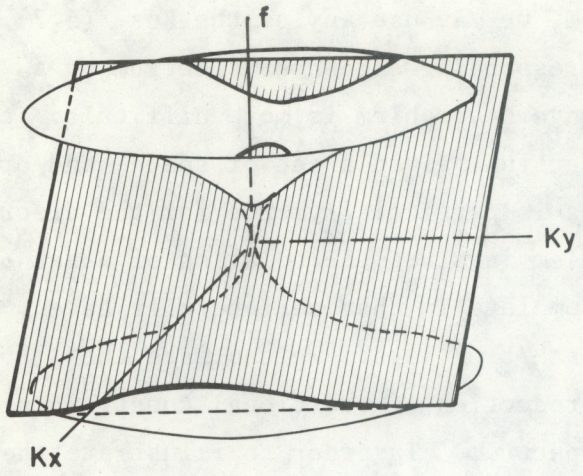

Figure 3. The effect of dispersion. For the discrete sensor case, contributions to encounter spectra arise only from the intersection of the encounter plane (shaded) and the dispersion surface (the unshaded paraboloid of revolution). The region inside a box centered on the origin is shown. The case illustrated corresponds to $0<f'/f_0<.25$. For linearly distributed sensors, the plane is replaced by a line that penetrates the dispersion surface at as many as four discrete wave numbers.

$$E''(f',K_y';\rho_i)=\int d\bar{K}F(K_x,K_y;f)\delta(f\pm\Omega)$$

$$\delta(K_y'-K_y+K_x\tan\Psi)\delta(f'-f-K_xU)e^{ik_x\rho_i}, \qquad (5.10)$$

and

$$F''(K_x',K_y';\tau_i)=\int d\bar{K}F(K_x,K_y;f)\delta(f\pm\Omega)$$

$$\delta(K_x'-K_x-\frac{f}{U})\delta(K_y'-K_y-\frac{f}{U}\tan\Psi)e^{i\omega\tau_i}. \qquad (5.11)$$

Geometrically, (5.7) and (5.8) mean that contributions to these one-dimensional encounter spectra arise only from surface wave numbers lying on the several branches of the curve defined by the intersection of the encounter plane and the dispersion surface (see Fig. 3). Thus, these two moments reduce to line integrals. Contributions to (5.9) through (5.11) arise only from the intersection of the line defined by the last two delta functions in each integrand with the dispersion surface. Thus, these moments reduce to the weighted sum of as many as four discrete values of $F(K_x,K_y;f)$.

6. SPECIFIC CASES

Given the surface wave spectrum, we may use any of the Eqs. (5.7) through (5.11) to calculate the corresponding encounter spectrum by a straightforward integration. The inverse problem is more difficult: to calculate the corresponding wave spectrum, given a set of space- and/or time-lagged encounter spectra. This is particularly true for the discrete sensor case, where the inverse problem involves the solution of a set of integral equations. The set is incomplete in that we generally have encounter spectra for only a few space/time lags. We can make the problem determinate only by the introduction of additional constraints on the nature of the surface wave spectrum. In order to illustrate the difficulties involved in the inverse problem and to suggest ways of dealing with them, we shall consider the cases corresponding to (5.7) and (5.11) in some detail; these two are of particular interest, since they represent frequently encountered experimental situations (wave gage arrays in a finite current, non-scanning laser/radar altimeters translating at finite velocity, laterally scanning laser/radar altimeters and imaging radars translating at non-zero velocity, and stereophotography).

The case represented by (5.7) is most conveniently treated in polar coordinates. Accordingly, we substitute (5.5) and (5.6) into (3.11) and get, upon integrating over $0 \leq K \leq \infty$,

$$E'(f;\bar{r}_i) = \int_0^{2\pi} d\theta \int_{-\infty}^{\infty} df\, E(\theta,f;\kappa)\delta(f'-q) \; e^{-i2\pi\kappa r_i \cos(\theta-\alpha_i)} \tag{6.1}$$

where $q=f-\kappa U \cos\theta$, and α_i is the direction of the "initial" sensor displacement vector $\bar{r}_i \equiv (\rho_i,\sigma_i,0)$ relative to the x direction. To integrate out the remaining delta function, we must transform to q as one of the

integration variables, replacing either f or θ. In the deep water approximation, $\kappa=2\pi f^2/g$, and the relevant transformation Jacobians are

$$\frac{\partial(\theta,f)}{\partial(\theta,q)} = \frac{1}{(1-4\cos\theta\,\frac{q}{f_0})^{\frac{1}{2}}}, \quad f_0=\frac{g}{2\pi U}$$

and

$$\frac{\partial(\theta,f)}{\partial(q,f)} = \frac{f_0}{f^2\sin\theta}, \quad \theta=\arccos\left[\frac{f_0}{f^2}(f-q)\right] .$$

Transforming, and then carrying out the integration over both branches of the transform q=q(f) or q=q(θ) gives, after some manipulation,

$$E'(f';\bar{r}_i)=\int_0^{2\pi} d\theta\,\frac{H_i(\theta,f_-(\theta,f'))+H_i(\theta,f_+(\theta,f'))}{(1-4\cos\theta\,\frac{f'}{f_0})^{\frac{1}{2}}} \tag{6.2}$$

or, equivalently,

$$E'(f';\bar{r}_i)=\int_{\infty}^{\infty} df\,\frac{f_0[H_i(\theta(f,f'),f)+H_i(-\theta(f,f'),f)]}{f^2\sin\theta(f,f')}, \tag{6.3}$$

where

$$H_i(\theta,f)=E(\theta,f;\kappa)e^{-i\frac{\omega^2}{g}r_i\cos(\theta-\alpha_i)} ,$$

$$f_{\pm}(\theta,f')=\frac{f_0}{2\cos\theta}\left[1\pm(1-4\cos\theta\,\frac{f'}{f_0})^{\frac{1}{2}}\right] ,$$

$$\theta(f,f')=\arccos\left[\frac{f_0}{f^2}(f-f')\right] ,$$

and E(θ,f;H) is taken to be identically zero for $f=f_{\pm}(\theta,f')$ complex or θ=θ(f,f') imaginary (i.e., cos θ >1). Both integrands have singularities,

for (6.2) at $\theta = \arccos \frac{f_0}{4f'}$ and for (6.3) at $\cos\theta = \pm 1$, where one or the other transformation Jacobian diverges.

We may now introduce the additional constraints necessary to make the problem determinate by replacing $E(\theta,f;\kappa)$ by a model spectrum, $\hat{E}(\theta,f)$, having degrees of freedom less than or equal to the number of independent pieces of information in the set of space-lagged encounter spectra. An especially convenient representation uses a linear expansion in a finite set of basis functions, allowing the remaining integrations (6.2) and (6.3) to be executed and reducing the set of integral equations to a tractable set of algebraic equations that may subsequently be solved for the parameters of the model. Several examples of this procedure exist in the literature for the special case U=0 (e.g., a wave gage array in still water) and for a single moving sensor (e.g., one airborne non-scanning laser or radar altimeter). See, for example, Barber (1963), Gilchrist (1966), Barnett and Wilkerson (1967), and Snyder (1974). Snyder (1973), in considering a scanning laser altimeter, formulated a problem similar to the present one but derived results applicable only to the case of large U. In order to obtain results for unrestricted U, consider the following:

In general, Fourier analysis of a realizable data set provides estimates of $E'(f';\bar{r}_i)$ at evenly spaced discrete encounter frequencies, say $f'_\ell, -L \leq \ell \leq L$, and for the $J(J-1)+1$ initial displacement vectors $\bar{r}_i$. (Recall that J=number of instruments in the array.) We can make this explicit by writing

$$E'(f',\bar{r}_i)=E'_{i\ell},\ \ell = \text{integer closest to } f'/\Delta f'. \qquad (6.4)$$

But from (3.5) and(3.11),

$$E'(-f';\bar{r}_i)=[E'(f';\bar{r}_i)]^*$$

and

$$E'(f';-\bar{r}_i)=[E'(f';\bar{r}_i)]^*.$$

Consequently, we have only (L+1) $(\frac{J(J-1)}{2}+1)$ encounter spectral values that are independent. This establishes the upper limit on the number of degrees of freedom the model may have.

Suppose we consider a model that is step-wise discontinuous in f but continuous in θ, i.e., $\hat{E}(\theta,f)$ is assumed constant at fixed θ over frequency bands of width Δf. (The choice of a constant bandwidth Δf is notationally convenient but not necessary; a modest modification of the development below could accommodate a model with frequency-dependent bandwidths.) Its distribution in θ we represent by an expansion in a finite set of basis functions, $\phi_m(\theta)$, whence we take

$$\hat{E}(\theta,f)=\sum_{m=1}^{M} E_{mn}\phi_m(\theta), \tag{6.5}$$

where n is the integer closest to f/Δf. The constants E_{mn} are then the free parameters of the model. Entering (6.4) and (6.5) into (6.2) and (6.3), we get, after some algebra,

$$E'_{i\ell} = \sum_{n=1}^{N}\left(\sum_{m=1}^{M} E_{mn}I_{i\ell mn}\right) \tag{6.6}$$

where, from (6.2),

$$I_{i\ell mn}= \int_0^{2\pi} d\theta \left[\frac{G^{-}_{imn}(\theta,f_+(\theta,f'_\ell))+G^{-}_{imn}(\theta,f_-(\theta,f'_\ell)}{\left(1-4\cos\theta\,\frac{f'_\ell}{f_0}\right)^{\frac{1}{2}}} + \frac{G^{+}_{imn}(\theta,f_+(\theta,-f'_\ell))+G^{+}_{imn}(\theta,f_-(\theta,-f'_\ell))}{\left(1+4\cos\theta\,\frac{f'_\ell}{f_0}\right)^{\frac{1}{2}}}\right] \tag{6.7}$$

or, equivalently, from (6.3),

$$I_{i\ell mn} = \int_{f_n - \frac{\Delta f}{2}}^{f_n + \frac{\Delta f}{2}} df \; \frac{f_0}{f^2} \left[\frac{G^-_{imn}(\theta(f,f'_\ell),f) + G^-_{imn}(-\theta(f,f'_\ell),f)}{\left|\sin \theta(f,f'_\ell)\right|} \right.$$

$$\left. + \frac{G^+_{imn}(\theta(f,-f'_\ell),f) + G^+_{imn}(-\theta(f,-f'_\ell),f)}{\left|\sin \theta(f,-f'_\ell)\right|} \right] \qquad (6.8)$$

We have used the abbreviations

$$G^{\pm}_{imn}(\theta,f) = \begin{cases} \phi_m(\theta) e^{\pm i \frac{\omega^2}{g} r_i \cos(\theta - \alpha_i)}, \text{ for} \\ \quad f \text{ and } \theta \text{ real and } f_n - \frac{\Delta f}{2} < f < f_n + \frac{\Delta f}{2} \\ 0, \text{ otherwise .} \end{cases}$$

Further, we have taken $E(\theta,0;0) \equiv 0$ and used the fact that $E(\theta,-f;\kappa) = E(\theta+\pi,f;\kappa)$ to eliminate the E_{mn} for $n<0$.

The integrals (6.7) and (6.8) are constants determined by the array geometry and the choice of basis functions, ϕ_m, and frequency sets, $f_n = n\Delta f$ and $f'_\ell = \ell \Delta f'$. They are alternate ways of evaluating the coefficients of the linear problem (6.6). Both formulas are necessary because each integrand is singular for some combinations of n and ℓ; whenever this difficulty arises with one formula (indicating a breakdown of the transformation from f or θ to q), the other is called into service to compute the coefficient for that band. If $U \neq 0$, (6.8) is the more convenient form, except for the bands in which $\theta(f,f') \to 0$ or $\pm\pi$, for which (6.7) must be used; in general, the integrals must be evaluated numerically, and if Δf is sufficiently small and the ϕ_m sufficiently smooth, the numerical integration may be approximated by the single term Δf times

the integrand evaluated at f_n. No such simplification is appropriate with (6.7) because the θ ranges contributing vary in size from one n to another and are not necessarily small.

Note that, in general, (6.6) involves the entire set of data points and model parameters in a single matrix problem. Important simplifications occur for the special case U=0, for which (6.7) reduces to

$$I_{i\ell mn} = \begin{cases} \int_0^{2\pi} d\theta\ \phi_m(\theta) e^{-i\frac{(2\pi f_n)^2}{g} r_i \cos(\theta-\alpha_i)}, \\ \qquad\qquad \text{for } f_n - \frac{\Delta f}{2} < f'_\ell < f_n + \frac{\Delta f}{2} \\ 0, \text{ otherwise} \end{cases}$$

and, hence, (6.6) is just

$$E'_{i\ell} = \sum_{m=1}^{M} E_{mn}\ I_{i\ell mn}$$

with n fixed by the value of f'_ℓ. Thus, the surface wave frequencies are decoupled, and the single MNxMN matrix problem decomposes into N MxM matrix problems, numerically much less troublesome to deal with. The question then arises: Under what conditions on U may we neglect a slow translation of our array relative to the water for the sake of the simpler formulation above?

A qualitative answer can be had by comparing the exact integration contour defined by the delta function in (6.1) with the approximate one obtained by letting U→0. The equation for the exact contour in (f,θ) space is (for deep water)

$$f' = f - \left(\frac{2\pi U}{g} \cos\theta\right) f^2 .$$

The several branches of the curve are plotted in Fig. 4. As $U \to 0$, the term in f^2 vanishes and the contours become circles. We may safely treat the problem as if $U \equiv 0$, provided the exact contour for a given f' does not deviate significantly from the circle $f' = f$ anywhere within the region in (f,θ) where significant surface wave spectral density exists. The test, then, consists of estimating the directional range of the surface wave field and the highest frequency with significant spectral density, and then verifying that $\left|\frac{2\pi U \cos\theta}{g} f^2\right|$ is no larger than one or two times Δf for that frequency and range of θ values.

Other, more familiar results for particular instrument geometries can be obtained from (6.5) through (6.8) in a reasonably straightforward way. For example, a procedure that has been used for dealing with records obtained with a single, non-scanning laser/radar altimeter is to choose for the basis function set, $\phi_m(\theta)$, a single assumed spreading factor for each surface wave frequency band (which may differ from one band to the next). The equivalent model is established in (6.5) through (6.8) by, e.g., setting $i=1$, $\bar{r}_i = 0$, and $\phi_m = 0$ for $m \neq n$. We may further choose each $\phi_n(\theta)$ to be normalized so that its integral over 2π radians equals unity; then (6.6) reduces to an NxN matrix problem for the discrete surface wave frequency spectral values, E_{nn}. This is essentially the procedure used by Barnett and Wilkerson (1967) (except that they invoked the additional simplifying assumption that no waves propagate upwind or outrun the translating sensor). For some of their calculations, they chose a totally unidirectional model, $\phi_n = \delta(\theta - \theta_w)$, where θ_w is the wind direction. We can show that the use of this choice in (6.7) and the assumption that no wave outruns the sensor will reduce (6.6) to a one-to-one correspondence between encounter spectrum and wave frequency spectrum,

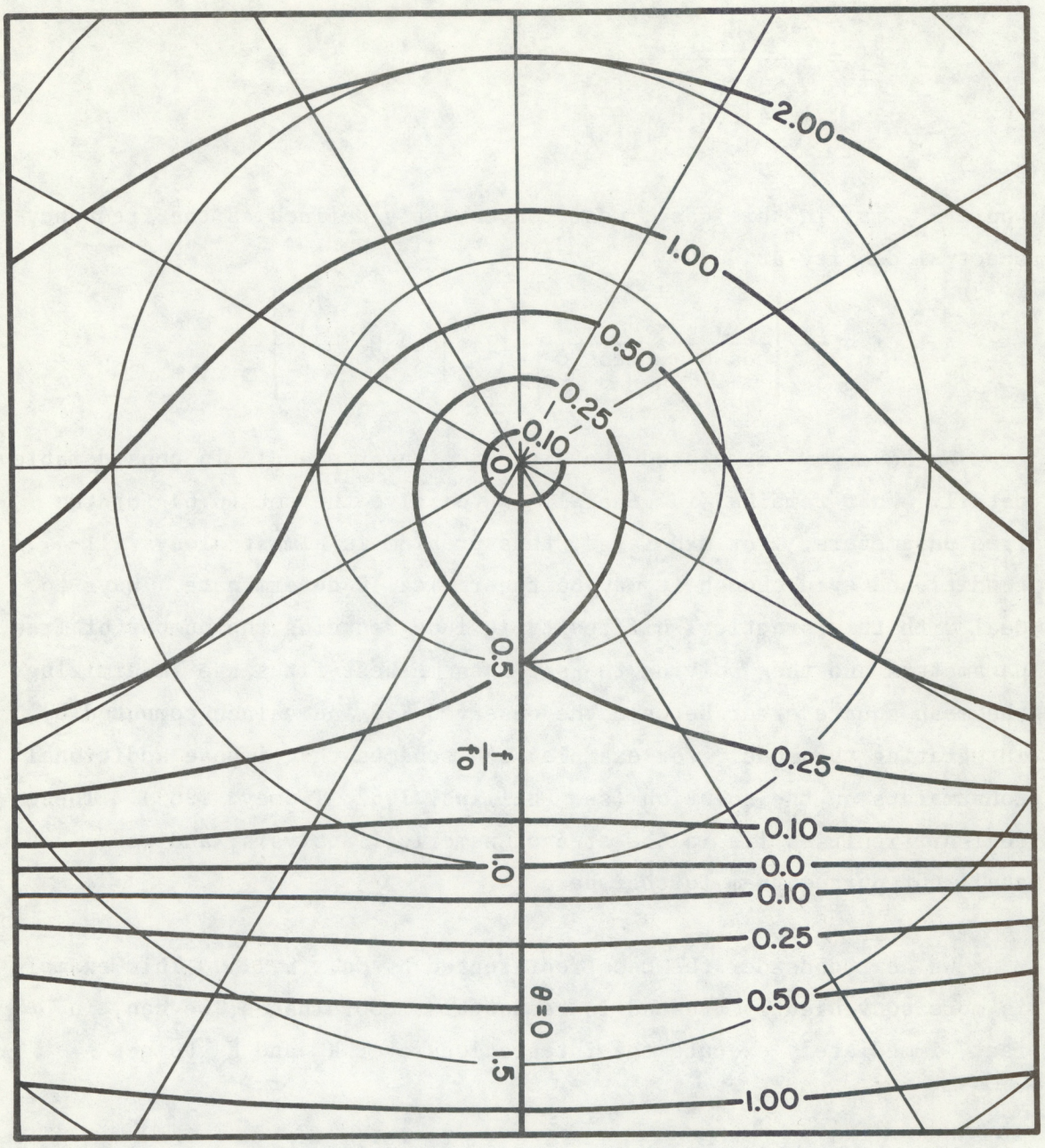

Figure 4. Integration contours for discrete sensors. The contours of this figure are obtained by projecting the lines of intersection of the encounter plane and the dispersion surface shown in Fig. 3 onto the (K_x, K_y) plane, and then mapping the result from (K_x, K_y) into (f,θ). Each contour is labeled with the corresponding value of f/f_0. θ is wave propagation direction relative to the translation direction, and the radial coordinate is f/f_0. The contour has three branches for $0<f'/f_0<0.25$, two for $f'/f_0<0.25$. See also Cartwright; 1963, St. Denis and Pierson, 1953.)

$$E'_{i\ell} = \frac{E_{nn}}{\left(1+4\left|\cos\theta_w\right|\frac{f'_\ell}{f_0}\right)^{\frac{1}{2}}}$$

where E_{nn} is, in this case, most conveniently defined as the frequency spectral density at

$$f_n = \frac{f_0}{2}\left[\frac{1}{\cos\theta_w} + \frac{1}{\left|\cos\theta_w\right|}\left(1+4\left|\cos\theta_w\right|\frac{f'_\ell}{f}\right)^{\frac{1}{2}}\right]$$

We have now formulated the discrete sensor example in considerable detail. What remains, in general, is to solve the set (6.6) for the free parameters. For MxN large, this problem is almost always ill-conditioned even though it may be theoretically determinate. Ways to deal with this practical difficulty include reducing the number of free parameters and then solving the set in some best-fit sense (minimizing the mean square error between the observed $E'_{i\ell}$ and values computed by integrating the model, for example) and schemes that impose additional constraints on the solution (see Phillips, 1962; Twomey, 1963). These real difficulties lie in the area of numerical analysis, and we shall not pursue them further here.

We next consider the case represented by Eq. (5.11). This example is more conveniently treated in rectangular coordinates; we can, in fact, immediately execute the integrations over K_x and K_y to get

$$F''(K'_x,K'_y;\tau_i)=\int_{-\infty}^{\infty} dfF(K_x,K_y;f)\delta(f\pm\Omega)e^{i\omega\tau_i}$$

where

$$\begin{cases} K_x = K'_x - \dfrac{f}{U} \\ K_y = K'_y - \dfrac{f}{U}\tan\Psi. \end{cases} \tag{6.9}$$

To integrate out the remaining delta functions, we must transform from f to

$$q_{\pm}=f\pm\Omega$$

as the integration variable; when the deep water approximation (5.2) for Ω is used, the transformation Jacobian is

$$\frac{\partial(f)}{\partial(q_{\pm})}=\left[1+\frac{1}{2}\,(\pm K^{-3/2})\,\left(\frac{g}{2\pi U^2}\right)^{1/2}(K_x+K_y\tan\Psi)\right]^{-1}\quad .$$

Transforming, and then carrying out the integration over all branches of $q_{\pm}=q_{\pm}(f)$, we get a contribution to the integral for each value of f for which $q_{\pm}=0$, whence

$$F''(K_x',K_y';\tau_i)=\sum_{p=1}^{4} J_p F(K_x,K_y;f_p)e^{i\omega_p\tau_i} \tag{6.10}$$

where

$$J_p=\begin{cases}\left|1+\frac{1}{2}\frac{f_0^2}{f_p^3}(K_xU+K_yU\tan\Psi)\right|^{-1}, & f_p \text{ real}\\ 0, & f_p \text{ complex},\end{cases} \tag{6.11}$$

and f_p, p=1,2,3,4, are the four roots of $q_{\pm}=0$, equivalent to the quartic equation

$$f^4=f_0^2\left[(K_x'U-f)^2+(K_y'U-f\tan\Psi)^2\right]\quad . \tag{6.12}$$

Thus, there may be as many as four surface wave components contributing to encounter spectral density at (K_x',K_y'). To parcel out the observed encounter spectral density among the several contributing surface wave numbers, we may need $F''(K_x',K_y';\tau_i)$ for as many as four distinct values of τ_i . But for moderately large U, only two of the

roots of (6.12) are important, the others being either complex or so small that the spectral density of these very long waves may safely be assumed zero. Then, only two distinct τ_i would be sufficient. In most real-life cases, only one τ_i is available, $\tau_i=0$. (Formations of aircraft bearing scanning altimeters or imaging radars are difficult to assemble.) In that case, some additional assumption must be made to make the problem determinate; we may, for example, prohibit the existence of waves propagating in the upwind semicircle of directions.

Nice simplifications are possible if we can treat the record as though it were acquired instantly. In our formulation this is equivalent to letting $U\to\infty$, in which case $J_p\to 1$ for the real roots of (6.12); moreover, from (6.9), $K_x=K'_x$ and $K_y=K'_y$, whence (6.12) reduces to

$$f^4=\left(\frac{g}{2\pi}\right)^2 \quad K'^2_x+K'^2_y \quad .$$

This has only two real distinct roots, $f=\pm\left(\frac{gK'}{2\pi}\right)^{\frac{1}{2}}$, corresponding to waves of wavelength $1/K'$ propagating antiparallel and parallel to (K'_x,K'_y). Choosing the sign corresponding to propagation in the downwind semicircle of directions is generally sufficient to reduce (6.10) to a one-to-one equivalence between encounter and surface wave spectra. This treatment ignores the refraction-like effects of finite U, which result in contributions to $F''(K'_x,K'_y;\tau_i)$ from surface wave numbers $(K_x,K_y)\neq(K'_x,K'_y)$ and a transformation Jacobian $\neq 1$.

As one might expect, the error occurring from neglect of the finite U effect is a function of the ratio C/U, where C is the surface wave phase speed. We can, in fact, rewrite (6.11) in the form

$$J_p=\begin{cases}\left|1-\frac{1}{2}\frac{|C|}{U}(\cos\theta+\sin\theta\tan\Psi)\right|^{-1}, C=\frac{f_p}{K(f_p)} \text{ real} \\ 0, \text{ otherwise}\end{cases} \qquad (6.13)$$

where θ is the direction of propagation of the surface wave defined, through (6.9), by K'_x, K'_y, and f_p. Moreover, this contribution to encounter spectral density will appear at an apparent propagation direction θ', which from (6.9) we can show to be

$$\theta' = \arctan\left[\frac{\sin\theta - \frac{|C|}{U}\tan\Psi}{\cos\theta - \frac{|C|}{U}}\right] , \qquad (6.14)$$

and at an apparent wavelength

$$\frac{1}{K'} = \frac{1}{K}\left|1-2\,\frac{|C|}{U}(\cos\theta+\sin\theta\tan\Psi)+\left(\frac{C}{U}\right)^2\sec^2\Psi\right|^{-\frac{1}{2}}. \qquad (6.15)$$

Thus, if $\frac{|C|}{U}<<1$ for the longest surface wave with significant spectral density, we may safely ignore the finite U effects and treat the images acquired by translating linearly distributed sensors as if they were acquired instantly.

7. CONCLUSIONS

Arrays of suitable discrete or linearly distributed instruments translating at constant velocity provide one- or two-dimensional records of sea surface elevation. Cross-spectral analyses of such record sets yield encounter spectra that are, in fact, integral properties of the full two-dimensional surface wave spectrum. We have derived these integral relationships in Eqs. (5.7) through (5.11) and provided a geometrical interpretation of the derivations. The problem of extracting an estimate of the surface wave spectrum, given a corresponding set of encounter spectra, has been treated in detail for cases corresponding to wave gage arrays in a current, in Eqs. (6.6) through (6.8), and to arrays of laterally scanning surface-imaging devices, in Eqs. (6.9) through (6.12). These detailed results reduce under limiting conditions U=0 or ∞ to well-known and much simpler forms, and we have provided a means of evaluating the effects of using these simpler versions (instead of the more exact but much more complicated forms) for any given problem.

8. REFERENCES

Barber, N. F. (1963): The directional resolving power of an array of wave detectors. In Ocean Wave Spectra. Prentice-Hall, Inc., Englewood Cliffs, N.J., 137-150.

Barnett, T. P., and J. C. Wilkerson (1967): On the generation of wind waves as inferred from airborne radar measurements of fetch limited spectra. J. Mar. Res., 25: 292-328.

Cartwright, D. E. (1963): The use of directional spectra in studying the output of a wave recorder on a moving ship. In Ocean Wave Spectra. Prentice-Hall, Inc., Englewood Cliffs, N.J., 203-218.

Gilchrist, A. W. R. (1966): The directional spectrum of ocean waves: an experimental investigation of certain predictions of the Miles-Phillips theory of wave generation. J. Fluid Mech., 25: 795-816.

Kinsman, B. (1965): Wind Waves; Their Generation and Propagation on the Ocean Surface. Prentice-Hall, Inc., Englewood Cliffs, N.J., 676 pp.

Phillips, D. L. (1962): A technique for the numerical solution of certain integral equations of the first kind. J. Assoc. Comput. Mach., 9: 84-97.

Pierson, W. J. (1975): The theory and applications of ocean wave measuring systems at and below the sea surface, on the land, from aircraft and from spacecraft. City University of New York report to Goddard Space Flight Center. 388 pp.

Snyder, R. L. (1973): On the estimation of the directional spectrum of surface gravity waves from a programmed aircraft altimeter. J. Geophys. Res., 78: 1475-1478.

Snyder, R. L. (1974): A field study of wave-induced pressure fluctuations above surface gravity waves. J. Mar. Res., 32: 497-531.

St. Denis, M., and W. J. Pierson (1953): On the motions of ships in confused seas. Trans. Soc. Nav. Archit. and Mar. Eng., 61: 280-357.

Twomey, S. (1963): On the numerical solution of Fredholm integral equations of the first kind by the inversion of a linear system produced by quadrature. J. Assoc. Comput. Mach., 10:97-101.